Al-Mustansiriyah Journal of Science
ISSN: 1814-635X (print) 2521-3520 (electronic)

ORIGINAL ARTICLE OPEN ACCESS

Synthesis of Cu-SnO_3 NCs by Photo Irradiation Method for Removal Tartrazine Dye Yellow in Aqueous Solutions

Saad Khalaf Madlool [a], Wafaa Mahdi Salih [a], and Ahmed Mahdi Rheima [b]

[a] Department of Physics, College of Science, Mustansiriyah University, Baghdad, Iraq
[b] Department of Chemistry, College of Science, Mustansiriyah University, Baghdad, Iraq

CORRESPONDENCE
Saad Khalaf Madlool
saadkhalaf79@yahoo.com

ARTICLE INFO
Received: October 09, 2023
Revised: February 13, 2024
Accepted: February 21, 2024
Published:September 30, 2024

ABSTRACT: ***Background:*** *Copper tin oxide (Cu-SnO_3) is a cheap and easily accessible tunable that has a 2.5-5 eV bandgap. It is a desirable semiconductor because of these components for a number of applications, including transparent conducting oxides, transistors, solar cells and photocatalytic.* ***Objective:*** *The aim of this research is to increase the rate of yellow dye removal percentage efficiency by using Photo Irradiation Method that rate was determined between (59 to 76) % by the simple chemical method.* ***Methods:*** *Photo irradiation method used to synthesis Cu-SnO_3 from precursor materials, the solution is irradiated by photocell for 30min with cooling (5°C) then drop sodium hydroxide (4 g in 100 ml) then washed, isolated by centrifugation for 20 minutes, grinding the dried powder and calcinated at (450 °C).* ***Results:*** *The crystallite size and the crystal structure of Cu-SnO_3 NPs are (43-8.2) nm with a tetragonal structure. Field Emission-Scanning Electron Microscopy (FESEM) results displayed the formation of spherical and semispherical and an average size of (35.97 - 74.43) nm. The optical energy gap value (Eg) is 5 eV. It is clear from the disappearance of tartrazine's yellow hue in an aqueous solution that the combination was shaken at 298 K and 185 rpm.* ***Conclusions:*** *Prove that the removal percentage process by a photo-irradiation method is more effective than other used methods.*

KEYWORDS: *Copper tin oxide; Photo irradiation method; Tartrazine dye yellow; Copper nitrate; Tin chloride dihydrate*

INTRODUCTION

Photo-irradiation, or the exposure to photo-energy emitted by electromagnetic rays, has been used as a human activity from the dawn of time. Its origins may be traced back to the ancient Egyptians, who employed it in mummification [1]. The simple process of photo irradiation is brought about by the absorption of light stimuli (as non-ionizing radiation energy), which increases the energy of the reactant molecule to a level suitable for chemical reactions [2]. This absorbed energy is adequate to initiate/promote a chemical reaction or to carry out crosslinking activity. Nanocomposites are widely used materials in a variety of applications, including batteries, fuel cells, photovoltaic cells, flexible cells, and photodegradation catalysis [3]. Nanophysics is a new growing discipline in physics, particularly in solid state physics, that focuses on the investigation and development of methods for producing usable materials with nanoscale dimensions (1-100 nm). The nanotechnology revolution in chemistry has led to the development of an environment conducive to collaboration among chemists and other professionals. Until it established collaboration with matter and industry experts, it worked in the domains of physics, biology, and engineering [3], [4]. Green synthesis of nanoparticles is more advantageous including reduction agent, stabilization, and most production of nanoparticles [5].

Nanoparticles NPs are the most important constituents of nanotechnology in structural masses [6]. NPs are tiny atomic or partial groups consisting of a particular number of atoms with diameters ranging from 1-100 nm and manufactured from organic or inorganic materials. When compared to produced and bulk materials, they exhibit unique features [7], [8]. Metal NPs have grown in popularity among the various NPs; their nature is distinct due to their exceptionally high aspect ratio. Iron

oxide nanoparticles have become increasingly important due to their environmental friendliness [9], [10], catalytic activity [11], [12], cheap cost [13], [14], and biocompatibility [15]. Because of their availability, resilience, and large surface area, copper oxide, tin oxide, and iron oxide NPs are also beneficial. They also have a wide range of uses in dye sensitized [16].

Copper oxide (CuO) and tin (II) oxide (SnO_2) nanoparticles (NPs) are important materials with significant future advantages over other materials [17], including special physiochemical properties, low toxicity, high catalytic activity, small volumes, high surface area to volume ratio, physical and magnetic properties [18].

Tarrazine, a synthetic lemon yellow azo dye, is largely used as a food colour. With the exception of green S (E142), tartrazine is a widely used hue throughout the world, particularly for yellow. It can also be blended with bright blue FCF (FD and C Blue 1, E133) or green S (E142) to generate various hues of green. Azoic derivatives are the most significant class of dyes [19]. In this work, CuO-SnO_3 NCs were produced using the photo-irradiation method. The purpose of this research is to find high purity, tiny particle size, and a big energy band gap for environmental treatments, as well as to live a safe life. This nanoparticle was characterized by UV-visible absorption spectra of each sample were measured using a spectrophotometer (SYSTRONICS DOUBLE BEAM UV-Vis Spectrometer) and the XRD to determine the structure properties by PANalytical X'Pert PRO, Netherlands) in University of Mansoura, Republic of Egypt. These NPs were validated by their use in dye absorption at various concentrations.

MATERIALS AND METHODS

Synthesis Cu-SnO_3 by Photo-irradiation Method

In order to prepare a solution, 2.41 grams of $Cu(NO_3)_2$ were dissolved in 50 milliliters of deionized water. Subsequently, 3.507 grams of $SnCl_4.6(H_2O)$ substances were solubilized in 50 milliliters of deionized water. The resulting solutions were mixed in the same beaker. Urea was then added to the mixture and allowed to react for one hour. The concentration of urea used was 2.4 grams per 100 milliliters of solution. The solution was irradiated by photocell for 30min with cooling (5 °C) then drop sodium hydroxide (4 g in 100 ml) and wash the precipitate three times, the precipitate was isolated by centrifugation for 20 minutes and dried and grinding the dried powder and calcinated at (450 °C). In this study, a cell was employed to subject the salt of tin and copper to irradiation, thereby serving as the precursor for the synthesis of nanostructures of CuO, SnO_2, and Cu-SnO_3. UV source (photolysis cell with power of 125 watt) was used, it consists of a medium-pressure ultraviolet lamp, the maximum wavelength of which is 365nm, and the power of the lamp is 125 watts. It is immersed in Pyrex reactor to withstand the heat. The cell contains a tube of quartz instead of ordinary glass because it does not absorb UV rays. The cell must be under continuous cooling to ensure that the reaction is in the same direction as photosynthesis not thermal.

Adsorption

To examine the adsorption behavior, several batch experiments were carried out of Tartrazine yellow dye onto nanoparticles of Cu-SnO_3. Each metal oxide nanoparticle (Cu-SnO_3) was added in the amount of 0.01 g to 10 ml of dye solution at varying concentrations (5, 10, 15, 20, and 25 ppm). The mixture was subjected to agitation using a water bath shaker, operating at predetermined parameters of speed, time, and temperature. Subsequently, centrifugation was employed at 500 rpm for adoration of 5 minutes to effect separation of the supernatant. The residual concentrations of dye were measured using a UV-Vis Spectrophotometer. The removal percentage (R%) and the quantity of dye adsorbed (qe) were computed using the following equations:

$$R\% = 100\left[\frac{C_i - C_e}{C_i}\right] \tag{1}$$

$$qe = V\frac{[C_i - C_e]}{m} \tag{2}$$

Where: The parameter qe (mg/g) represents the quantity of dye that has been adsorbed onto nanoparticles at a state of equilibrium. Ci and Ce denote the initial concentration and the concentration at equilibrium, respectively, measured in milligrams per liter (mg/L). V refers to the volume of the working solution, measured in liters (L), while m represents the mass of the nanoparticles, measured in grams (g).

Characterization

The impact concerning various parameters, like effects time, the nanoparticles mass, starting adsorbate concentrations and temperature were studied in this work. The impact of adsorption duration on the efficacy of Tartrazine yellow dye removal. which was carried out at temperatures 298K, adsorption time (30-45) minutes, the concentrations were 10 mg/L for dye volume was 10 ml, nanoparticles mass was 0.01 g and shaking speed was 185 rpm.

The effect of adsorbent dosage on dye adsorption has been examined at different amounts of nanoparticles dosage (0.01, 0.05, 0.1, and 0.15 g). These experiments were performed in four volumetric flasks containing 10 ml of starting concentration of 10 mg/L for dye. The adsorption time was 30 minutes temperatures of 298 K for dye, and the shaking speed was 185 rpm. The effect of starting dye concentrations was carried out at a temperature of 298K for dye. The concentrations were (5, 10, 15, 20 and 25) mg/L of dye, the volume was 10 ml and adsorbent dosage of 0.01g and 10 ml of dye, the shaking time was 30 minutes for the dye, and the shaking speed was 185 rpm.

Five different temperatures were applied to determine the preferable temperature for the adsorption of dye onto nanoparticles (288, 298, 308, 318 and 328) K. The amount of nanoparticles was 0.01g. Therefore, the volume was 10 ml of 10 mg/L of dye solution, the shaking time was 30 minutes for the dye and shaking speed was 185 rpm.

Isotherm study was carried out by taking a 10 ml volume of dye solution with 10 mg/L starting concentrations of Tartrazine yellow dye solution, at temperatures (298) K, in a set of volumetric flasks.. Whereas for kinetics study, a dye solution of 10 ml at 298 K was used in a set of volumetric flasks. All the volumetric flasks were placed in a thermostatic water bath shaker and stirred to the equilibrium time for 75 minutes for the dye. 5 ml was drawn from the supernatant during this time, each 5, 10, 15, 20 and 25 minutes for the dye till reaching the equilibrium time. To separate liquid and solid phases, the suspension solutions were centrifuged for 5 minutes at 3500 rpm. The transparent liquid was subjected to analysis via a UV-Vis spectrophotometer, with a focus on the maximum wavelength of 425 nm, in order to investigate the various adsorption isotherms and kinetic models of the dye. spectroscopy (Biotech Engineering Management). In the wavenumber domain, the instrument operates (400-4000) cm^{-1}. A contact angle measuring was used (digital microscope 500x-1000x magnification ratio, China) at room temperature, and used droplets of(5μL) Deionized water. Image j software was used to measure the contact angle.

RESULTS AND DISCUSSION

XRD analysis of (Cu-SnO_3) NCs

In order to investigate the crystal structure type and crystalline size of prepared(Cu-SnO_3) NCs, an X-ray diffraction (XRD) examination was conducted using a simple chemical method at a calcination temperature of 450. The results are presented in Figures 1-6, which displays the XRD patterns of (Cu-SnO_3) NCs synthesized through a photo method. The presented illustration depicts the development of a face-centered-cubic crystal structure, characterized by a space group of (Pm3m), crystal dimensions of (a = b = c = 9.4 A°), and crystal angles of $\alpha = \beta = \gamma = 90°$. This structure corresponds to the face center cubic structure (JCPDS 00-001-1117) [20].

Cu-SnO_3 NCs made using a photo-irradiation technique are shown in Figure 1 with their XRD patterns. In order to comprehend potential Cu-SnO_3, the observed characteristic peaks at copper demonstrated the establishment of face center cubic crystal structure (JCPDS, copper file no. 04-0836). Cu (311), Cu (220), and Cu (202) were utilized as structural models, whereas SnO_3 in the Cu-SnO_3 represented the SnO_3 (110), SnO_3 (101), and SnO_3 (211), corresponding to (27°), (39°), and (55°), as seen in Figures 2, and which corresponds to the tetragonal structure (JCPDS 00-041-1445). It is notices in this result that a shift occurs with an increase in intensity and less crystal size compared to the Figure 3. There is no comparable reference and this outcome has never been achieved by originality.

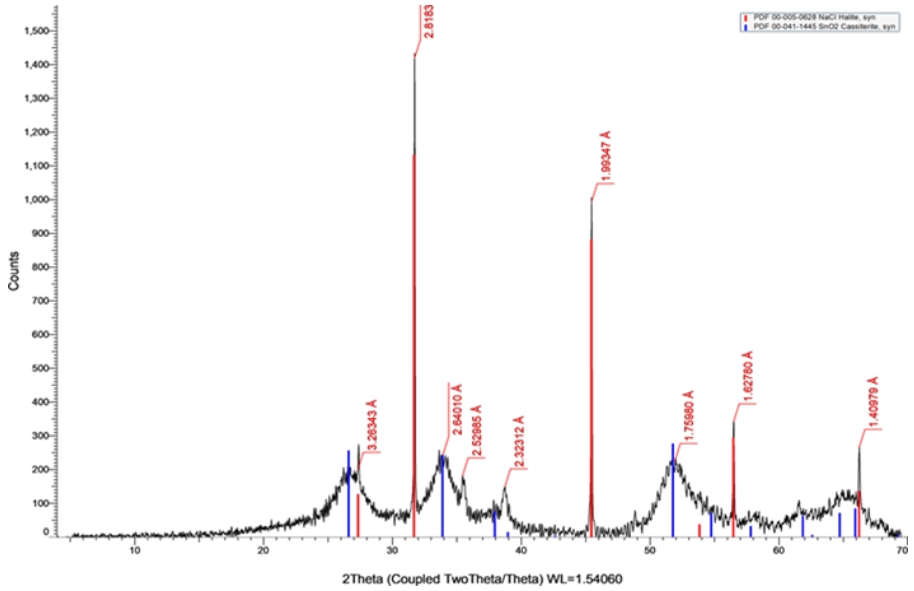

Figure 1. XRD patterns of Cu-SnO_3 NCs prepared via photo-irradiation method

FE-SEM of Cu-SnO_3 NCs

The particle size and shape of Cu-SnO_3 NCs are depicted in Figure 2 (a, b). Cu-SnO_3 NCs have a smaller particle size than CuO. Cu-SnO_3 NCs have a large spherical shape.

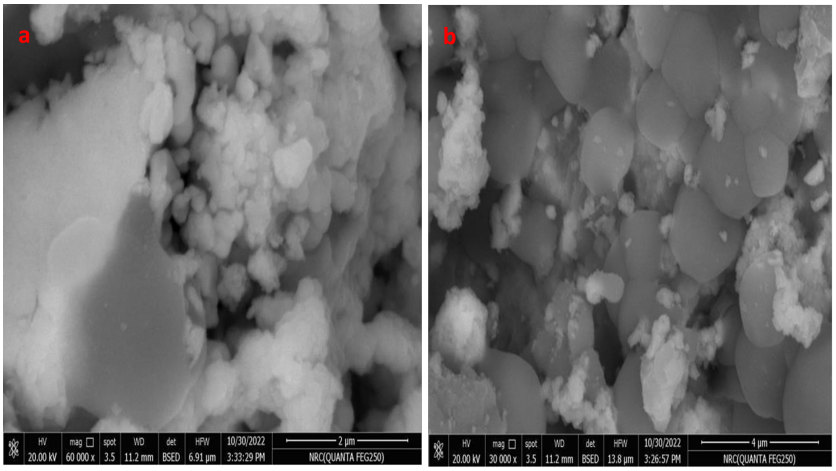

Figure 2. FE-SEM images of Cu-SnO_3 NCs

EDX and mapping of Cu-SnO_3 NCs

The Sn and O atomic contents of SnO_2 NPs are lower than the predicted values (33:67) of stoichiometric SnO_2 NPs agree with [19] as it demonstrated in Figure 3 which shows a Cu peak with a high Cu content at wt 41.37 % or 35.55 Cu loading, but wt 45.91 % or at 21 % is still less than that of Sn.

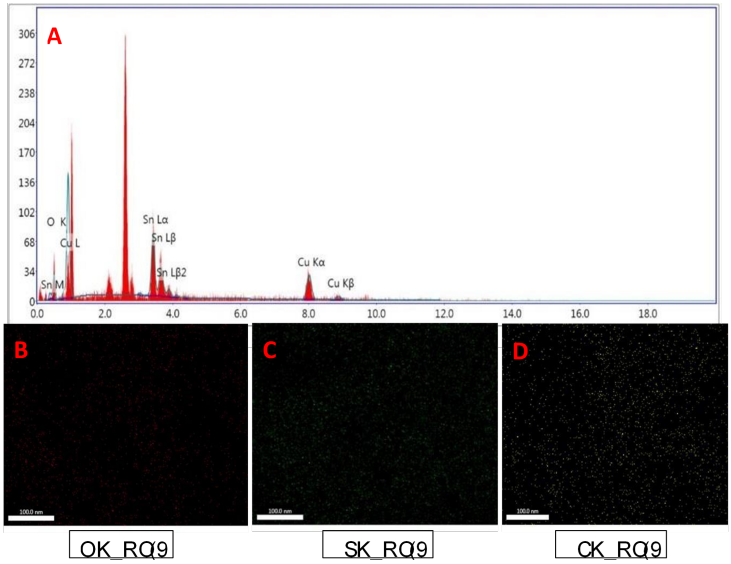

Figure 3. The means and SD of Ca in control, RA and OA

TEM analysis of Cu-SnO_3 NCs preparation by the photo method

TEM images were utilized to assess the sample's shape and average particle size as it is illustrated in Figure 4A. The image shows that, with the exception of a few aggregated particles, spherical nanoparticles were produced and uniformly distributed. Copper Tin oxide (Cu-SnO_3) NCs have a diameter that is estimated from TEM images to be between ±3.3 to 4.2 nm [19]. When used the photo irradiation method notices an increase in purity, and accuracy. The photo-irradiation technique is characterized by a significant reduction in the average grain size of particles within a crystal. This is attributed to the splitting of particles resulting from their collision with thermal energy generated by irradiation. This feature is considered to be of utmost importance in the context of this technique.

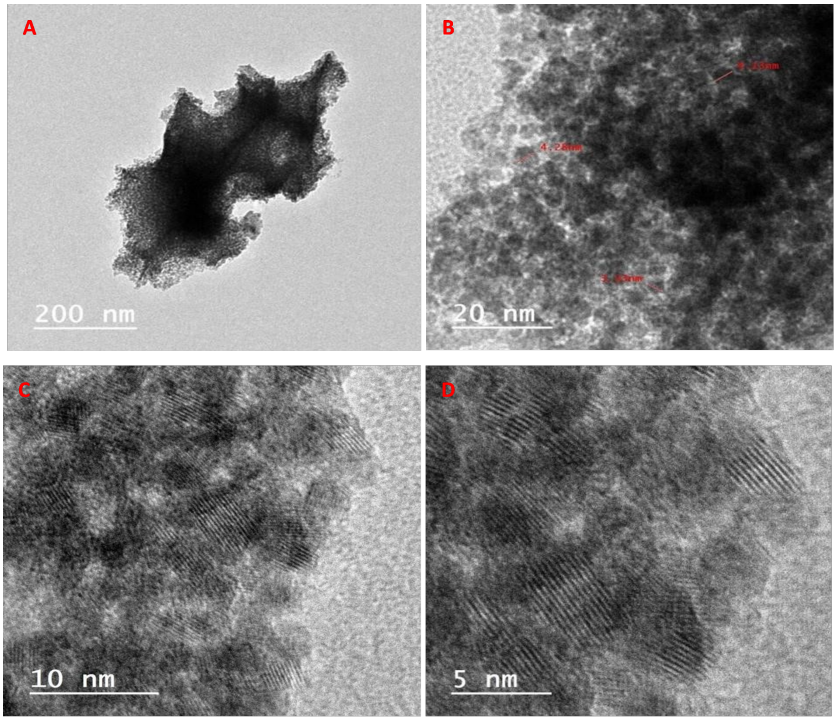

Figure 4. TEM analysis shows the nanostructure of shape Cu-SnO_3 NCs

UV-Visible Spectrometer of Cu-SnO_3 NPs Preparation by Photo- Irradiation Method

The optical transmittance spectra of, (Cu-SnO_3) NPs using at 450 by photo irradiation method as is shown in Figure 5. All films exhibit an elevation in transmittance beyond 400nm wavelengths (> 80%) in the visible region, commonly referred to as the transparent window for light. The aforementioned phenomenon is ascribed to the films' substantial absorbance within this particular region, which corresponds with the optical properties of (CuO) metal in the UV-Vis spectrum. Conversely, a significant decrease in the T % of the films is observed in the cut-off region, where wavelengths dip below 400nm (< 80%).

This is due to the films' intense absorbance in this region [20], [21]. The various material thicknesses utilized to make the films result in a broad range of absorbance variations among them all. The films' significant absorption in this area is consistent with the metal SnO_2 optical properties in the UV-Vis spectrum [22]. The optical transmittance spectra of (Cu-SnO_3) NCs produced using a photo irradiation method approach at (450) °C.

XRD measurements of changes in average crystallite size, dislocation density, and microstrain can be used to explain variations in the optical band gap. Figure 6 displays the optical band gap values determined by a straightforward photo irradiation process at 450 °C and the range value is (5 eV),respectively.

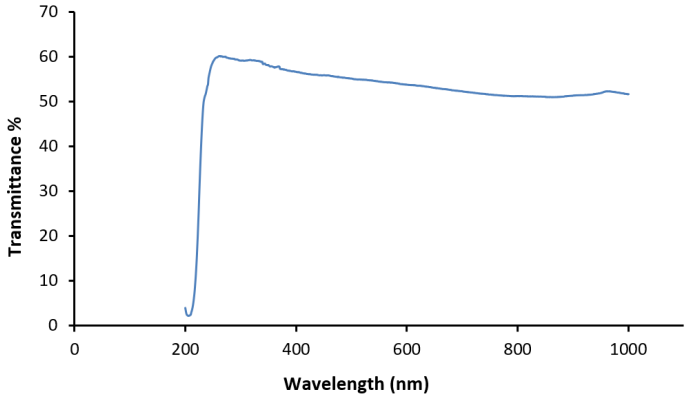

Figure 5. UV-visible spectrum shows the transmittance of Cu-SnO_3 NCs

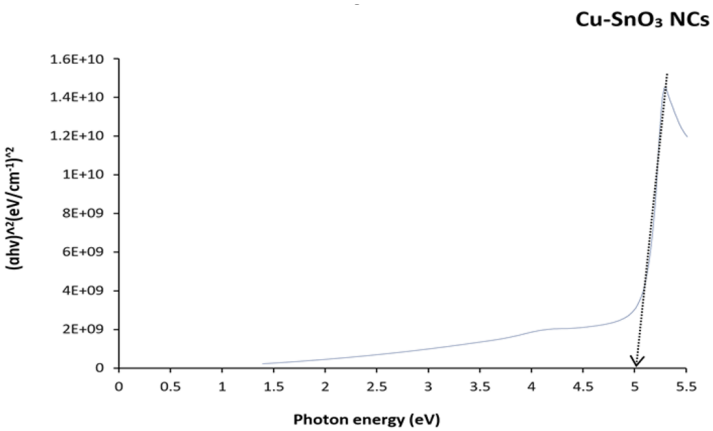

Figure 6. Energy gap of Cu-SnO_3 NCs

Adsorption of Dye on the Surface of Cu-SnO_3 NCs

The Preparation of direct yellow dye (tetazron) to measure the absorption spectrum and study the calibration curve was registered using a UV-visible spectrophotometer at a maximum wavelength of 430 nm. Figure 7 shows the UV-visible spectrum.

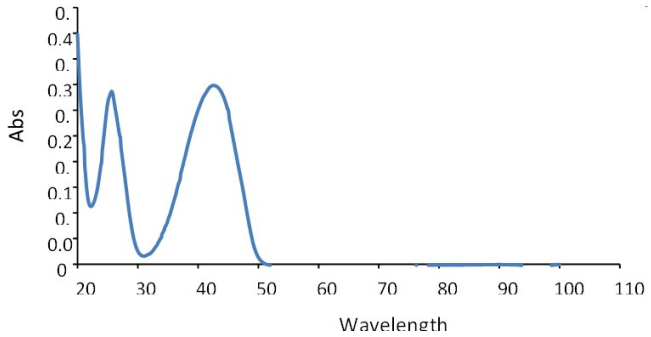

Figure 7. UV-visible absorption spectrum of direct yellow dye

1 Effect of Contact Time

The amount of adsorption increases directly with the increase in the concentration of the dye and then reaches a steady state at 60 minutes as shown in Figure 8. This may be due to the vacant adsorption sites on the surface of the nanoparticle, which then slowly increase until the time reaches 60 minutes to reach equilibrium [23].

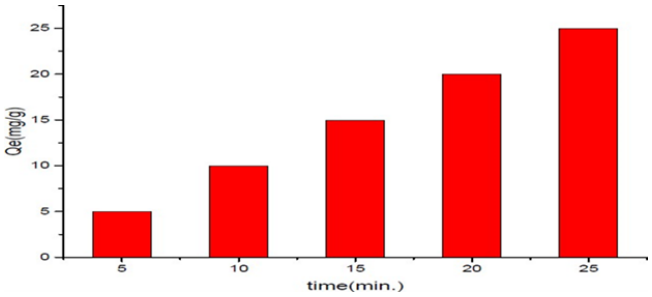

Figure 8. Effect of time on adsorption of dye onto the Cu-SnO_3 NCs

2 The Mass Effect of Cu-SnO_3 NCs Preparation by the Photo-Irradiation Method

To study the effect of mass for Cu-SnO_3 NCs preparation by the photo-irradiation method on the dye (4-43) the removal percentage by nanoparticle increased from 59% to 76%, with the increase in nanoparticle mass. At first, the adsorption rate is rapid due to the increased active site of Cu-SnO_3 NCs nanoparticle. Then, increased adsorption of dye was shown by increasing the amount of adsorbent mass. Thus, at a high mass, the Cu-SnO_3 NCs provides more active surface sites [24] as it is shown in Figure 9.

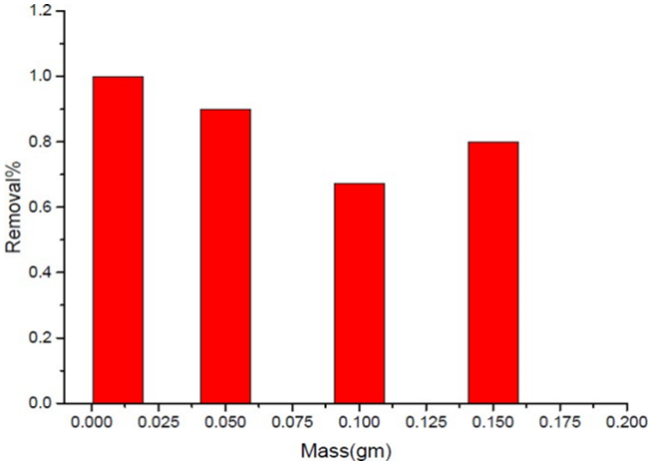

Figure 9. Effect of time on adsorption of dye onto the Cu-SnO_3 NCs

3 Effect of Temperature

The effect of temperature on the dye removal percentage by altering the temperature from 288 K to 328K under optimal conditions. According to reports, the removal rate increases with increasing temperature. This reflects the endothermic nature of the adsorption process. In addition, increasing temperature causes the internal structure to expand, thus large dye molecules penetrate onto Cu-SnO_3 NCs preparation by the photo-irradiation method surface [25].

Adsorption Isotherms

The adsorption isotherm can determine the type of interaction between the adsorbent and the adsorbate and the probability of the entire adsorption process [26]. It deals with the connection between the surface of the adsorbent and the liquid state when equilibrium is reached at a constant temperature. The isotherm can be represented by a curve (qe vs Ce).

1 Langmuir Adsorption Isotherm

The Langmuir isotherm model posits that the maximum adsorption capacity is achieved when a saturated monolayer of solute molecules is present on the adsorbent surface [27]. The rate of adsorption exhibited a persistent trend, as evidenced by the linear equation of specific adsorption Ce, Qe versus Ce. Figure 10 shows the Langmuir isotherm plots for dye adsorption onto nanoparticle samples.

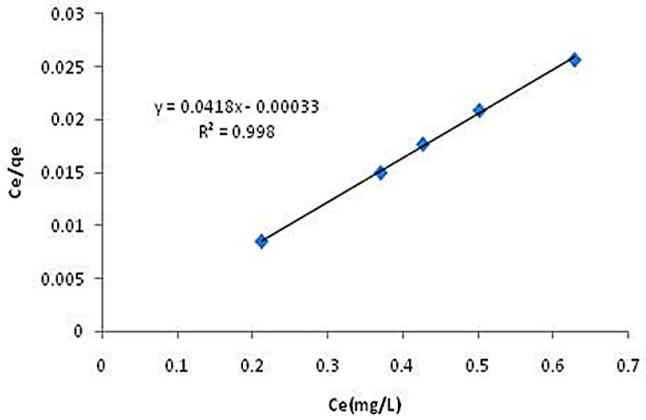

Figure 10. Langmuir isotherms of direct yellow dye at 318 K

2 Freundlich Adsorption Isotherm

Freundlich model assumes direct blue dye adsorption takes place on sites by various adsorption at heterogeneous nanoparticle surfaces and can be applied to multi-layer adsorption [28]. The values of these factors were estimated from the intercept and the slope of the graph between ln qe vs ln Ce, Figure 11 shows the Freundlich isotherm graphs for dye adsorption on the nanoparticle sample.

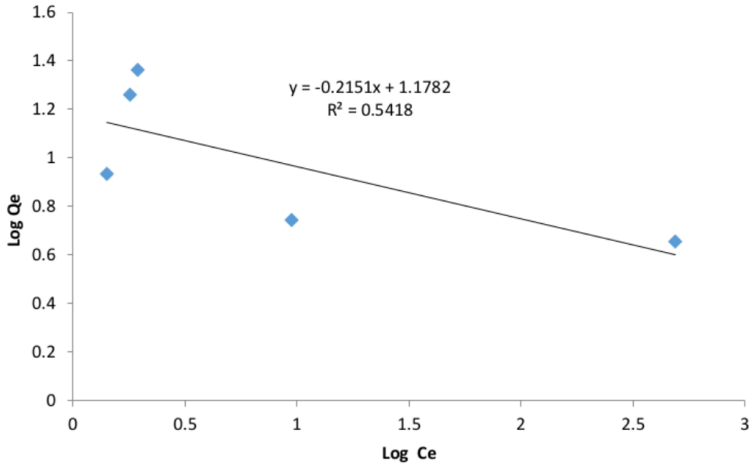

Figure 11. Freundlich isotherm model at 308 k

CONCLUSION

Cu-SnO_3 nanocomposites preparation at calcination temperature (450 °C) nanostructures successfully synthesized using the photo-irradiation method. The nanostructures are utilized for the examination of their structure and optical properties. This approach possesses attributes such as simplicity, cost-effectiveness, and environmental sustainability, thereby enabling the method to be economically feasible for the production of diverse high-quality nanostructures. The best results in this search were (8.2 to 43) nm of Cu-SnO_3 nanocomposites determined by X-ray diffraction analysis. FE-SEM images showed the grain size Cu-SnO_3 nanocomposites vie the value (35.97 - 74.43) nm. While TEM images clear the value of particle size is (5 - 65.04) nm. The optical band gap for Cu-SnO_3 nanocomposites was (5) eV. All nano-sized syntheses exhibited favorable structural properties, which were contingent upon various factors, including size, structure, surface roughness, and material impurities. The rate of yellow dye removal percentage efficiency is proved to be between (76 to 90)%. by photo-irradiation method. The removal percentage process of CuO NPs, SnO_2 NPs, and Cu-SnO_3 NCs with the effect of a photo-irradiation method is more effective than that of nano CuO NPs, SnO_2 NPs, and Cu-SnO_3 NCs by the simple chemical method.

SUPPLEMENTARY MATERIAL

None.

AUTHOR CONTRIBUTIONS

Saad Khalaf Madlool: Worked on the experimental part. Wafaa Mahdi Salih: Wrote the article. Ahmed Mahdi Rheima: Made the final procedures

FUNDING

None.

DATA AVAILABILITY STATEMENT

None.

ACKNOWLEDGMENTS

We are grateful to Mustansiriyah University, College of Science, Department of Physics for their valuable help.

CONFLICTS OF INTEREST

The authors declare no conflicts of interest.

REFERENCES

[1] M. Hallajiqomi and H. Eisazadeh, "Adsorption of manganese ion using polyaniline and it's nanocomposite: Kinetics and isotherm studies," *Journal of industrial and engineering chemistry*, vol. 55, pp. 191–197, 2017. doi: 10.1016/j.jiec.2017.06.045.

[2] A. Murugesan, M. Loganathan, P. Kumar, and D. Vo, "Cobalt and nickel oxides supported activated carbon as an effective photocatalysts for the degradation methylene blue dye from aquatic environment," *Sustainable Chemistry and Pharmacy*, vol. 21, p. 100 406, 2021. doi: 10.1016/j.scp.2021.100406.

[3] M. A. Abid and D. A. Kadhim, "Novel comparison of iron oxide nanoparticle preparation by mixing iron chloride with henna leaf extract with and without applied pulsed laser ablation for methylene blue degradation," *Journal of Environmental Chemical Engineering*, vol. 8, no. 5, p. 104 138, 2020. doi: 10.1016/j.jece.2020.104138.

[4] C. F. da Silva Ribeiro, A. Dionizio, T. Teodoro Araújo, C. M. Vilas Boas Feitosa Rodrigues, A. Costa Mattos, L. Galli Otaviano, L. Tercília Grizzo, A. C. Magalhães, and M. Afonso Rabelo Buzalaf, "Effect of experimental toothpaste containing hydroxyapatite nanoparticles and propolis, with and without fluoride, on the microcosm biofilm and enamel demineralization," *Biofouling*, pp. 1–10, 2023. doi: 10.1080/08927014.2023.2217689.

[5] M. A. Abid, D. A. Kadhim, and W. J. Aziz, "Iron oxide nanoparticle synthesis using trigonella and tomato extracts and their antibacterial activity," *Materials Technology*, vol. 37, no. 8, pp. 547–554, 2022. doi: 10.1080/10667857.2020.1863572.

[6] M. A. Albrecht, C. W. Evans, and C. L. Raston, "Green chemistry and the health implications of nanoparticles," *Green chemistry*, vol. 8, no. 5, pp. 417–432, 2006. doi: 10.1039/b517131h.

[7] L. LaConte, N. Nitin, and G. Bao, "Magnetic nanoparticle probes," *Materials today*, vol. 8, no. 5, pp. 32–38, 2005. doi: 10.1016/S1369-7021(05)00893-X.

[8] K. N. Thakkar, S. S. Mhatre, and R. Y. Parikh, "Biological synthesis of metallic nanoparticles," *Nanomedicine: nanotechnology, biology and medicine*, vol. 6, no. 2, pp. 257–262, 2010. doi: 10.1016/j.nano.2009.07.002.

[9] M. Senthil and C. Ramesh, "Biogenic synthesis of fe_3o_4 nanoparticles using tridax procumbens leaf extract and its antibacterial activity on pseudomonas aeruginosa," *Digest Journal of Nanomaterials & Biostructures (DJNB)*, vol. 7, no. 4, 2012.

[10] S. Venkateswarlu, Y. S. Rao, T. Balaji, B. Prathima, and N. V. V. Jyothi, "Biogenic synthesis of fe_3o_4 magnetic nanoparticles using plantain peel extract," *Materials Letters*, vol. 100, pp. 241–244, 2013. doi: 10.1016/j.matlet.2013.03.018.

[11] A. Kumar Das, A. Marwal, and R. Verma, "Bio-reductive synthesis and characterization of plant protein coated magnetite nanoparticles," *Nano Hybrids*, vol. 7, pp. 69–86, 2014. doi: 10.4028/www.scientific.net/NH.7.69.

[12] F. Luo, Z. Chen, M. Megharaj, and R. Naidu, "Biomolecules in grape leaf extract involved in onestep synthesis of iron-based nanoparticles," *RSC Advances*, vol. 4, no. 96, pp. 53 467–74, 2014. doi: 10.1039/C4RA08808E.

[13] S. Venkateswarlu, B. N. Kumar, C. H. Prasad, P. Venkateswarlu, and N. Jyothi, "Bio-inspired green synthesis of fe_3o_4 spherical magnetic nanoparticles using syzygium cumini seed extract," *Physica B: Condensed Matter*, vol. 449, pp. 67–71, 2014. doi: 10.1016/j.physb.2014.04.031.

[14] K. S. Siddiqi, A. ur Rahman, Tajuddin, and A. Husen, "Biogenic fabrication of iron/iron oxide nanoparticles and their application," *Nanoscale research letters*, vol. 11, no. 1, p. 498, 2016. doi: 10.1186/s11671-016-1714-0.

[15] D. A. Kadhim, M. A. Abid, and W. M. Salih, "Study the degradation and photocatalytic activity of the methylene blue dye by mixing the aloe vera extract with rust iron oxide nanoparticle," *Natural Resources for Human Health*, vol. 3, no. 3, pp. 355–363, 2023. doi: 10.53365/nrfhh/170025.

[16] H. Kumar, "A review on facile synthesis of nanoparticles made from biomass wastes," *Nanotechnology for Environmental Engineering*, vol. 7, no. 3, pp. 783–796, 2022. doi: 10.1007/s41204-022-00259-9.

[17] D. Singh, D. Jain, D. Rajpurohit, G. Jat, H. S. Kushwaha, A. Singh, S. R. Mohanty, M. K. Al-Sadoon, W. Zaman, and S. K. Upadhyay, "Bacteria assisted green synthesis of copper oxide nanoparticles and their potential applications as antimicrobial agents and plant growth stimulants," *Frontiers in Chemistry*, vol. 11, p. 1 154 128, 2023. doi: 10.3389/fchem.2023.1154128.

[18] W. J. Aziz, M. A. Abid, D. A. Kadhim, and M. K. Mejbel, "Synthesis of iron oxide (β-fe_2o_3) nanoparticles from iraqi grapes extract and its biomedical application," in *IOP Conference Series: Materials Science and Engineering*, vol. 881, 2020, p. 012 099. doi: 10.1088/1757-899X/881/1/012099.

[19] K. Karthik, V. Revathi, and T. Tatarchuk, "Microwave-assisted green synthesis of sno_2 nanoparticles and their optical and photocatalytic properties," *Molecular Crystals and Liquid Crystals*, vol. 671, pp. 17–23, 2018. doi: 10.1080/15421406.2018.1542080.

[20] A. B. Ali Baig, V. Rathinam, and V. Ramya, "Synthesis and investigation of fe doped sno_2 nanoparticles for improved photocatalytic activity under visible light and antibacterial performances," *Materials Technology*, vol. 36, no. 10, pp. 623–635, 2021. doi: 10.1080/10667857.2020.1786781.

[21] N. Jayaprakash, R. Suresh, S. Rajalakshmi, E. Sundaravadivel, and S. Raja, "One-step synthesis of cuo nanoparticles and their effects on h9c2 cardiomyoblasts cells," *Inorganic and Nano-Metal Chemistry*, vol. 50, no. 8, pp. 644–653, 2020. doi: 10.1080/24701556.2020.1723628.

[22] B. Bai, S. Saranya, V. Dheepaasri, S. Muniasamy, N. S. Alharbi, B. Selvaraj, V. S. Undal, and B. M. Gnanamangai, "Biosynthesized copper oxide nanoparticles (cuo nps) enhances the anti-biofilm efficacy against k. pneumoniae and s. aureus," *Journal of King Saud University-Science*, vol. 34, no. 6, p. 102 120, 2022. doi: 10.1016/j.jksus.2022.102120.

[23] S. T. Nipa, R. Akter, A. Raihan, S. b. Rasul, U. Som, S. Ahmed, J. Alam, M. R. Khan, S. Enzo, and W. Rahman, "State-of-the-art biosynthesis of tin oxide nanoparticles by chemical precipitation method towards photocatalytic application," *Environmental Science and Pollution Research*, pp. 1–23, 2022. doi: 10.1007/s11356-021-17933-1.

[24] M. B. Mobarak, M. S. Hossain, F. Chowdhury, and S. Ahmed, "Synthesis and characterization of cuo nanoparticles utilizing waste fish scale and exploitation of xrd peak profile analysis for approximating the structural parameters," *Arabian Journal of Chemistry*, vol. 15, no. 10, p. 104 117, 2022. doi: 10.1016/j.arabjc.2022.104117.

[25] P. V. Viet, C. M. Thi, and L. V. Hieu, "The high photocatalytic activity of sno2 nanoparticles synthesized by hydrothermal method," *Journal of Nanomaterials*, 2016. doi: 10.1155/2016/4231046.

[26] D. Berra, S. E. Laouini, B. Benhaoua, M. R. Ouahrani, D. Berrani, and A. Rahal, "Green synthesis of copper oxide nanoparticles by pheonix dactylifera l leaves extract," *Digest Journal of Nanomaterials and Biostructures*, vol. 13, no. 4, pp. 1231–1238, 2018.

[27] S. Jillani, M. Jelani, N. U. Hassan, S. Ahmad, and M. Hafeez, "Synthesis, characterization and biological studies of copper oxide nanostructures," *Materials Research Express*, vol. 5, no. 4, p. 045 006, 2018. doi: 10.1088/2053-1591/aab864.

[28] A. Azam, S. S. Habib, N. A. Salah, and F. Ahmed, "Microwave-assisted synthesis of sno2 nanorods for oxygen gas sensing at room temperature," *International journal of nanomedicine*, pp. 3875–3882, 2013. doi: 10.2147/IJN.S51206.